Water Research 266 (2024) 122373

Contents lists available at ScienceDirect

Water Research

journal homepage: www.elsevier.com/locate/watres

Cathodic poised potential stimulated the electron-sensitive C-P lyase pathway in glyphosate biodegradation

Qingshi Wang [a], Jackson Boodry [b], Tahir Maqbool [a], Brandon C. Bukowski [b], Daqian Jiang [a,*]

[a] Department of Civil, Construction, and Environmental Engineering, The University of Alabama, Tuscaloosa, AL 35487, USA
[b] Department of Chemical and Biomolecular Engineering, Johns Hopkins University, Baltimore, MD 21218, USA

ARTICLE INFO

Keywords:
Bioelectrochemical system (BES)
Glyphosate degradation
Density functional theory (DFT)
Pathway thermodynamics
Geobacter lovleyi
Hydroxylamine reductase

ABSTRACT

Glyphosate, the most widely used herbicide globally, is accumulating in the environment and poses significant potential eco- and bio-toxicity risks. While natural attenuation of glyphosate has been reported, the efficacy varies considerably and the dominant metabolite, aminomethylphosphonic acid (AMPA), is potentially more persistent and toxic. This study investigated the bioelectrochemical system (BES) for glyphosate degradation under anaerobic, reductive conditions. Atomistic simulations using density functional theory (DFT) predicted increased thermodynamic favorability for the non-dominant C-P lyase degradation pathway under external charge, which suppressed AMPA production. Experimental results confirmed that cathodic poised potential (-0.4 V vs. Ag/AgCl) enhanced glyphosate degradation (75 % in BES vs. ~40 % in the control conditions after 37 days), and lowered the AMPA yield (0.52 mol AMPA yield per mol glyphosate removed in BES vs. 0.77–0.86 mol mol^{-1} in the control conditions). *Geobacter lovleyi* was likely the active species driving the C-P lyase pathway, as evidenced by the increase of its relative abundance, the upregulation of its extracellular electron transfer genes (most notably mtr) and the up-regulation of its *phnJ* and *hcp* genes (encoding C-P layse and hydroxylamine reductase respectively).

1. Introduction

Application of glyphosate [*N*-(phosphonomethyl)glycine], the most frequently used broad-spectrum herbicide globally (Sun et al., 2019), has increased 12-fold since 1995 (from 67 to 826 million kg annually) (Benbrook, 2016; Duke and Powles, 2008) due to its high effectiveness in weed control and low toxicity to non-target organisms (Benbrook, 2016). The intensive use has resulted in increasing environmental accumulation (Torretta et al., 2018), with concentrations up to hundreds mg/kg in soil (Ololade et al., 2014, 2019; Silva et al., 2018) and hundreds μg/L in water (Battaglin et al., 2014; European Food Safety Authority (EFSA), 2015), as well as detection in commercial animal feeds (Zhao et al., 2018). Unchecked glyphosate accumulation could have a host of adverse effects on water quality, soil quality and fertility (Romano-Armada et al., 2019), and humans (IARC, 2015).

Natural attenuation of glyphosate relies on microbial degradation through two aerobic pathways: the C-P lyase pathway and the glyphosate oxidoreductase pathway (Zhan et al., 2018). The latter typically dominates and produces aminomethylphosphonic acid (AMPA) (Grandcoin et al., 2017). AMPA could pose chronic health effects on animals and humans (Balbuena et al., 2015; Van Bruggen et al., 2018), and is generally considered more persistent than glyphosate under natural conditions (Imfeld et al., 2013) with half-life reported to be as high as non-degradable (Tang et al., 2019) to 240 days (Campanale et al., 2021) (although the persistence of AMPA is still being debated and some reported half-life between 10 days (Zhang et al., 2015) to 100 days (Bento et al., 2016)). A nationwide survey in the U.S. confirmed that AMPA was detected more frequently, at similar or higher concentrations than glyphosate in environmental samples (Scribner et al., 2007). There is an urgent need to develop new degradation processes that yield safer metabolites.

Bioelectrochemical system (BES) is a device that utilizes electroactive microbes and extra-cellular electron transfer to drive redox reactions (Pant et al., 2012; Wilberforce et al., 2021). As a biodegradation platform, BES has the unique capability to pinpoint oxidative (anodic) and reductive (cathodic) reactions given its fuel cell-like setup. On the cathode side, BES has demonstrated great versatility in using a variety of electron acceptors including H^+ (Logan et al., 2008), CrO_4^{2-} (Huang

Abbreviations: AMPA, Aminomethylphosphonic acid; BES, Bioelectrochemical system; DFT, Density functional theory.

* Corresponding author.
E-mail address: djiang6@ua.edu (D. Jiang).

https://doi.org/10.1016/j.watres.2024.122373
Received 1 May 2024; Received in revised form 27 August 2024; Accepted 1 September 2024
Available online 2 September 2024

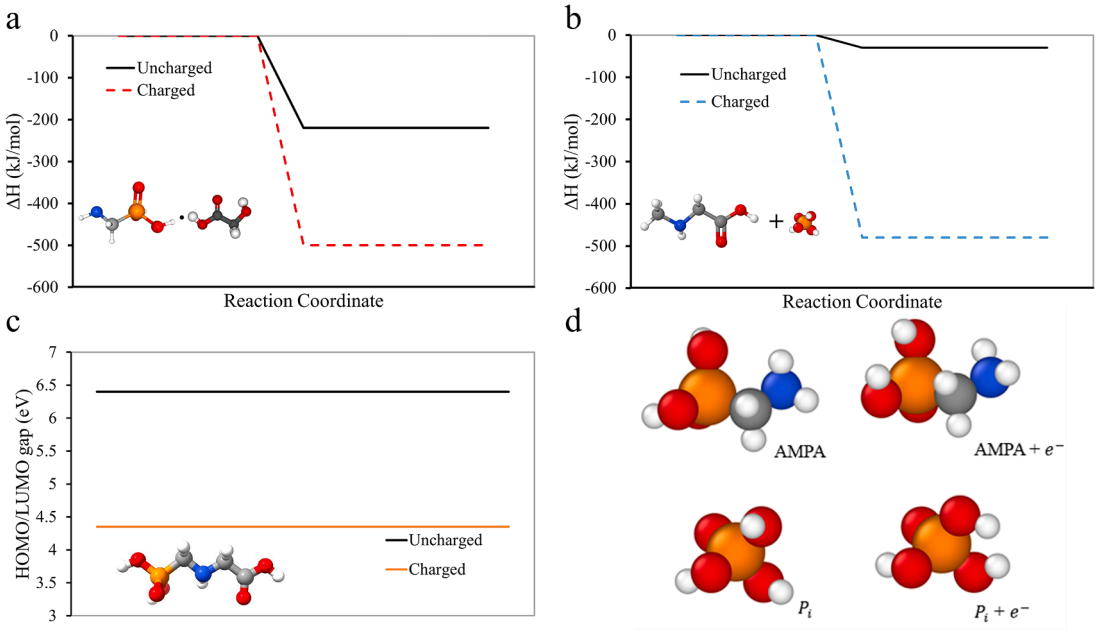

Fig. 1. Reaction coordinate diagrams for the AMPA and C-P lyase decomposition pathways (a and b respectively), HOMO/LUMO gaps for glyphosate with and without charge (c), and molecular structure of phosphorus decomposition products (d).

et al., 2015), CO_2 (Villano et al., 2010), nitrate (NO_3^-) and perchlorate (ClO_4^-) (Sevda et al., 2018). Further, BES was shown to have the capability of utilizing external voltage to augment reductive reactions (e.g., biohydrogen production (Logan et al., 2008)) or drive non-spontaneous reactions (e.g., CO_2 reduction (Villano et al., 2010)).

Given the relatively achievable theoretical energy for cleaving C-P and C-N bonds (264 kJ/mol and 305 kJ/mol respectively (Cottrell, 1958)) and binding energy for the glyphosate oxidoreductase–glyphosate, C–P-lyase–glyphosate, and C–P-lyase–AMPA complexes (−5.4 kcal/mol, −4.3 kcal/mol, and −5.1 kcal/mol respectively (Bhatt et al., 2021)), we hypothesized that BES could be exploited to manipulate glyphosate degradation. This approach synthesized glyphosate degradation techniques previously explored in the literature, particularly breakdown by microorganisms and abiotic electrochemical degradation (Musa et al., 2023; Zhan et al., 2018). Unlike the aerobic degradation reported so far, we targeted anaerobic reductive degradation under −0.4 V poised potential (vs. Ag/AgCl) in BES cathode. We combined theoretical simulation and experimental verification, in which we predicted the thermodynamic favorability and experimentally monitored glyphosate disappearance, metabolite generation (i.e., AMPA, sarcosine, glycine, phosphate), and microbial community compositions under three conditions: bioelectrochemical reduction, abiotic electrochemical reduction, and non-electric microbial degradation. Our goal was to confirm the viability of bioelectrochemical glyphosate degradation and to identify conditions and functional microbes that could achieve new glyphosate degradation pathways for real-world remediation applications.

2. Materials and methods

2.1. Density functional theory simulations

Initial molecular structures were generated for glyphosate as well as the decomposition products. Two pathways were considered: the AMPA pathway, which forms through cleaving the glyphosate C-N bond, and the C-P lyase pathway, formed by cleaving the C-P bond. *Ab-initio* simulations were performed using the ORCA package (Lehtola et al., 2018; Neese, 2018, 2012). Species were calculated in the charge neutral and 1^- charge state to simulate the stability of decomposition products under a strong applied potential. An initial geometry optimization at the BP86 (Becke, 1988) level of theory was performed before a final optimization at the B3LYP (Becke, 1993; Stephens et al., 1994) level to obtain the converged geometry. The Def2-TZVP basis set was used in each of these simulations, with a convergence criterion for the geometry optimizations of 3.0×10^{-4} Ha bohr^{-1} (Weigend and Ahlrichs, 2005). We performed single-point energy calculations at the M06 (Zhao and Truhlar, 2008) level to obtain reaction energies and HOMO/LUMO gaps.

We define the reaction enthalpy change (ΔH) of the AMPA and C-P lyase pathways as the difference in electronic energy described in Eq. (X).

$$\Delta H = E_{products} - E_{reactant} \quad \text{(X)}$$

Where the electronic energy of the reactant for both pathways is glyphosate, and the electronic energy of the products depend on the pathway. We calculated reaction energies for neutral glyphosate and each decomposition product, which are shown in the black lines of Fig. 1a and 1b. We then introduced an additional electron to each system to simulate the largest possible change expected in reaction thermodynamics where an applied potential could stabilize an additional electron on the reactants and products. This model was chosen to obtain a thermodynamic understanding of how sensitive each pathway is to an additional electron. We calculated the change in reaction enthalpy for both the AMPA pathway and C-P lyase pathway according to Eq. (Y)

$$\Delta\Delta H = \Delta H_{0^+} - \Delta H_{1^-} \quad \text{(Y)}$$

Where ΔH_{0^+} is the charge neutral reaction enthalpy, and ΔH_{1^-} is the reaction enthalpy after including an additional electron.

Charge transfer analysis is quantified here according to Eq. (Z)

$$\Delta Q_{atom} = Q_{atom,0^+} - Q_{atom,\ 1^-} \quad \text{(Z)}$$

Where $Q_{atom,\ 0^+}$ is the native Hirshfeld charge for a particular atom on the neutral molecule, and $Q_{atom,\ 1^-}$ is the Hirshfeld charge on an atom in the 1^- charged molecule.

2.2. Reactor construction, startup, and operation

Two-chamber bio-electrochemical reactors were constructed with acrylic sheets. Each chamber was 550 mL in volume and separated by a

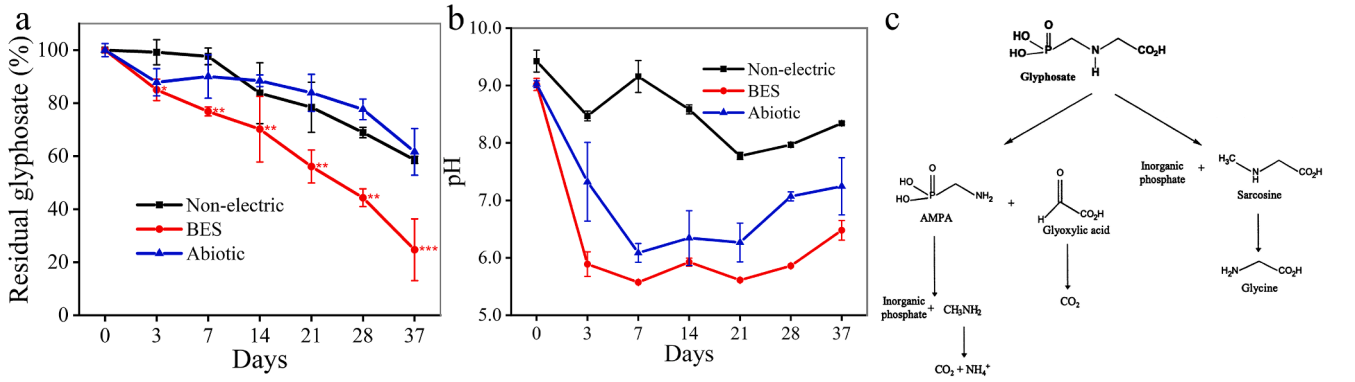

Fig. 2. Temporal profiles of glyphosate concentration and pH (a and b, respectively) and known glyphosate biodegradation pathways (c, recreated from the literature (Giesy et al., 2000)). "Non-electric", "BES", and "Abiotic" are the open circuit control, the BES treatment condition, and the abiotic control, respectively. $^{*}p < 0.05$, $^{**}p < 0.01$, $^{***}p < 0.001$.

Table 1
Comparison of the molar ratios of AMPA yield to glyphosate removal in this study and previous studies. Ratios were sometimes estimated based on figures and tables in previous studies.

Conditions (aerobic/ anaerobic)	Biomass	Mole AMPA yield per mole glyphosate removed	Refs.
Anaerobic, biological reduction (non-electric control)	Wastewater-sourced bacteria	0.77 ± 0.10	This study
Anaerobic, bio-electrochemical reduction	Wastewater-sourced bacteria	0.52 ± 0.05	This study
Anaerobic, electrochemical reduction	None	0.86 ± 0.04	This study
Aerobic degradation	Bacteria cell-free extracts	0.56	Fan et al. (2012)
Aerobic degradation	Bacteria cell-free extracts	0.75	Sviridov et al. (2012)
Aerobic biological degradation	Soil-sourced microbes	0.15 (1 sample) 0.75–0.92 (5 samples)	Tang et al. (2019)
Aerobic biological degradation	Sediment-sourced microbes	0.81 - –0.93	Tang et al. (2019)
Aerobic biological degradation	Pure culture *Pseudomonas* sp. strain LBr	0.95	Jacob et al. (1988)
Aerobic biological degradation	Pure culture *Geobacillus caldoxylosilyticus* T20 (thermophile)	1	Obojska et al. (2002)
Aerobic biological degradation	Soil-sourced bacteria	1	Hadi et al. (2013)
Aerobic biological degradation	Soli/aeration tank sourced fungi	1	Krzyśko-Lupicka et al. (1997), Fu et al. (2017)

CMI-7000S Cation Exchange Membrane (Membranes International, Inc., New Jersey, USA). The anode was 5 cm × 5 cm × 1 cm graphite sheet. The cathode was platinum mesh plate. The reference electrode was RE-5B Ag/AgCl electrode (Bioanalytical System, Inc., Indiana, USA). The poised potential was applied by a Model 1000C Series Multi-Potentiostat (CH Instruments, Inc., Texas, USA).

The electroactive biofilms were cultivated in the anodic mode with a poised potential of +0.2 V (vs. Ag/AgCl). The inoculum was wastewater from a local wastewater treatment plant (Tuscaloosa, AL, USA). The anode solution consisted of 10 mM phosphate buffer (pH = 7.8), 1 g/L sodium bicarbonate, 0.8 g/L sodium acetate, and vitamins and mineral salts as described elsewhere (Brandon et al., 2020). Anodes were inoculated with 30 % (v/v) wastewater to anode solution in the first three cycles and pure anode solution for three more cycles. Final anode solution was purged with nitrogen gas (purity N 99.9 %) for 10 min at 10 psi. The cathode solution was 10 mM phosphate buffer solution in each cycle. At the end of the cultivation phase, the peak current was 9.26 mA, and the Coulombic efficiency was 53.82–67.27 %.

Upon completion of the cultivation phase, the test phase was conducted in the cathodic mode. Four conditions were compared: the non-electric (open circuit) control, the non-glyphosate control, the BES treatment condition, and the abiotic control. Except for the non-electric control, −0.4 V (vs. Ag/AgCl) was applied; except for the non-glyphosate control, 5 mg/L glyphosate was added to the catholyte. The catholyte also contained 1 g/L sodium bicarbonate and 0.8 g/L sodium acetate. The anode solution was10 mM phosphate buffer solution (pH = 7.40). The reactors were operated for five weeks. All reactors were kept at room temperature (~25 °C) and sampling holes were covered with tape to minimize water evaporation throughout the experiments.

2.3. Metabolites and water quality measurements

Glyphosate, AMPA, sarcosine, and glycine were quantified by Agilent Ultivo Triple Quadrupole LC/MS/MS (Agilent Technologies, Inc., California, USA). Isotope-labelled glyphosate-2–13C was applied as an internal standard. 120 µl of 5 % borate buffer and 120 µl of 12 g/L 9-Fluorenylmethyl chloroformate (FMOC—Cl) were added to 1 ml of the sample and thoroughly shaken for 1 min. The derivatization process occurred at ambient temperature overnight, following which 120 µl of HCl was added to halt the derivatization reaction. Prior to measurement, the samples were filtered using a 0.45 µm filter. The mobile phases were prepared following method outlined by Sun et al. (2019) (Sun et al., 2019), optimized operating conditions and MRM parameters are provided in Appendix. pH was measured using the Ag/AgCl pH electrode (Thermo Fisher Scientific, Massachusetts, USA). Current generation was measured by the potentiostat (CH Instruments, Inc., Texas, USA) every 40 s.

2.4. DNA extraction, sequencing, and microbial community analysis

Biofilms were preserved at the end of the cultivation phase and the end of the test phase. DNA extraction of samples was performed using ZYMO *Quick*-DNA/RNA™ Microprep Plus Kit D7005 (Zymo Research, Irvine, CA, USA) according to the manufacturer's instructions. Samples were sequenced by Zymo Research (Irvine, CA, USA). The sequences reported in this article have been deposited in the NCBI BioProject (accession no PRJNA1066388). Gene annotations are from UniProt

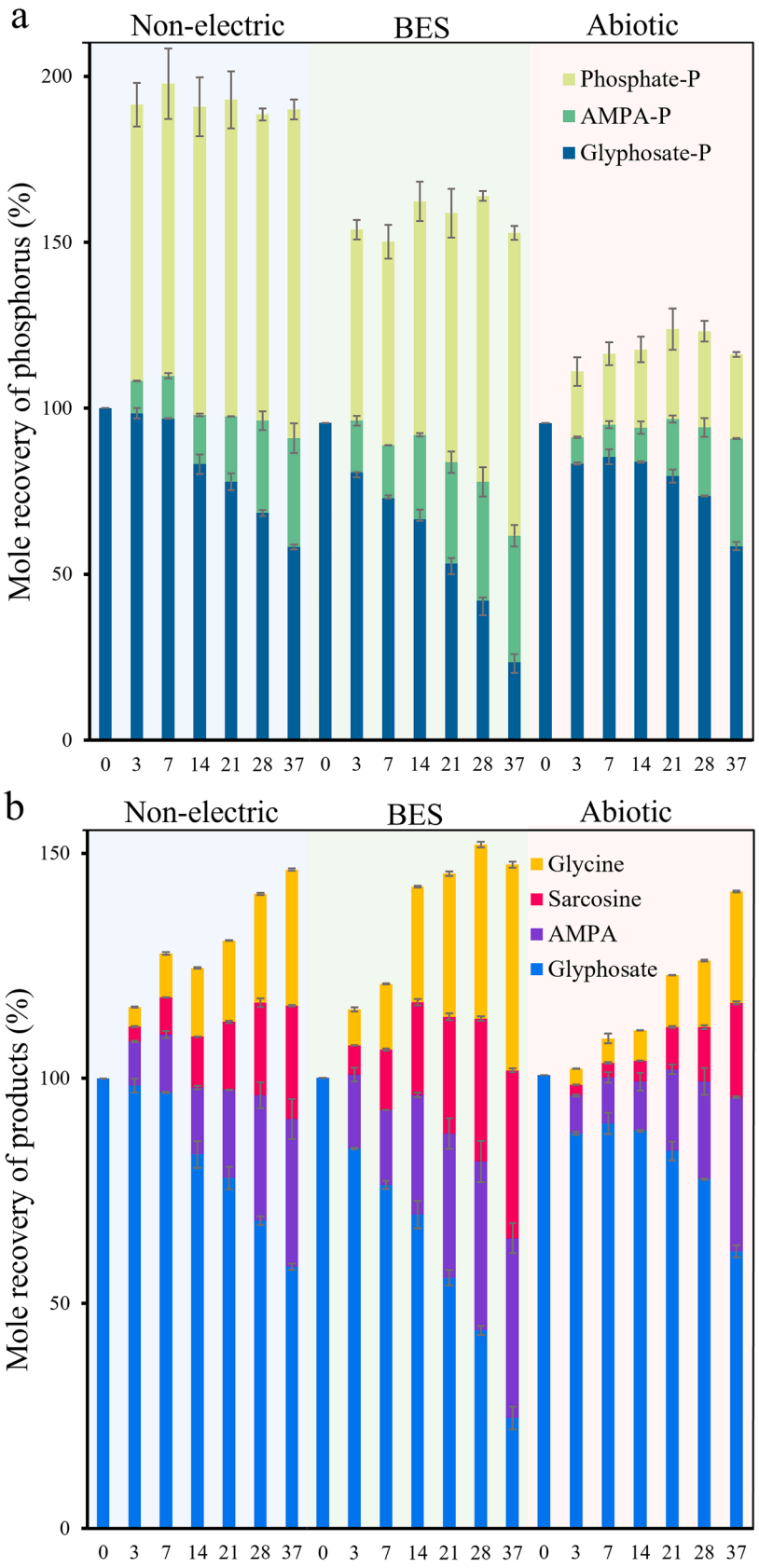

Fig. 3. Mole recovery of phosphorus (a) and degradation products (b). "Non-electric", "BES", and "Abiotic" are the open circuit control, the BES treatment condition, and the abiotic control, respectively.

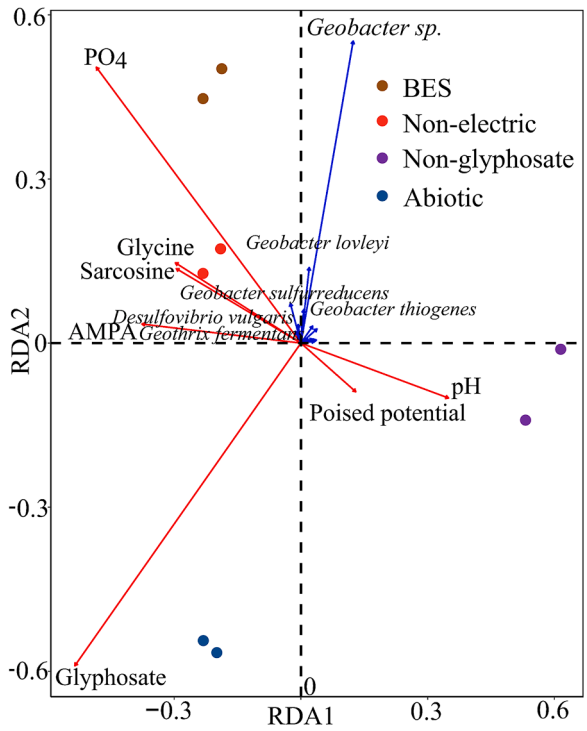

Fig. 4. Redundancy analysis (RDA) of reactor conditions and microbial community composition. "Non-electric", "BES", "Abiotic" and "Non-glyphosate" are the open circuit control, the BES treatment condition, the abiotic control, and the no-glyphosate control, respectively.

(https://www.uniprot.org/), the redundancy analysis (RDA) is performed with the community ecology package vegan of R 4.2.2.

3. Results and discussion

3.1. Simulated decomposition pathway thermodynamics

DFT calculations revealed a shift in the thermodynamic favorability across both decomposition pathways (Fig. 1a and 1b) upon applying an additional electron. We found that the change in reaction enthalpy ($\Delta\Delta H$) of the AMPA pathway decreased by 266 kJ/mol upon adding an additional charge, while the C-P lyase pathway saw a comparatively large change, decreasing by 435 kJ/mol. The reaction enthalpy was similar for charged and uncharged states across both AMPA and C-P lyase pathway (ΔH_{1^-} =499 and ΔH_{0^+} =457 kJ/mol) for these pathways, respectively. Reaction diagrams are shown in Fig. 1a and 1b. Given the similar enthalpy change across both pathways, it is plausible that similar quantities of AMPA and C-P lyase would be produced if the system were to fully equilibrate with an applied potential and that both pathways were kinetically accessible. The negative shift in reaction enthalpy across both pathways implies that the addition of an extra electron leads to glyphosate decomposition becoming more thermodynamically favorable, regardless of pathway.

The shift in the HOMO/LUMO gap of glyphosate indicates decreased thermodynamic stability after adding an additional electron. The HOMO/LUMO gap of neutral glyphosate was calculated to be 6.43 eV. Upon adding charge, this shifted to 4.26 eV, representing a decrease of 2.17 eV (Fig. 1c). Generally, a high HOMO/LUMO gap is correlated with increased molecular stability, meaning the added charge on glyphosate reduces the HOMO/LUMO gap magnitude and decreases its thermodynamic stability (Kosar and Albayrak, 2011).

The localization of the location of the added electron amongst the decomposition products was determined by analyzing the relative thermodynamic stability of these molecules with an added charge. In either case, it was found that the phosphorus decomposition product had a lower total energy. The difference in energy amongst charged decomposition products for the AMPA and C-P lyase pathways were 236.28 and 13.02 kJ/mol, respectively. The comparatively low energetic difference between charged species for the C-P lyase pathway could help explain the benefits of the applied potential, since either decomposition product is relatively stable with the added electron compared to the AMPA case. Still, an added charge on either phosphorus decomposition product results in significant conformational change in the molecule (Fig. 1d). This is most evident in analyzing changes in the P-O-H bond angle for either compound. For the AMPA pathway, the average P-O-H bond angle increased from 108.4° to 111.1° upon adding an electron, while in the C-P lyase pathway this angle increased from 106.6° to 112.3°. Hirshfeld charge transfer analysis revealed significantly increased electron density amongst the hydrogen atoms bonded to the phosphorus groups in both pathways. In the AMPA pathway, $\Delta Q_{H,\ avg} = -0.24\ e$ while the C-P lyase pathway saw slightly increased charge transfer to these hydrogens with $\Delta Q_{H,\ avg} = -0.27\ e$.

3.2. Cathodic poised potential facilitated glyphosate degradation

The experimental results agreed with the DFT predictions. First off, glyphosate degradation under the BES treatment conditions was significantly faster than both the non-electric and abiotic control conditions (Fig. 2a, $p < 0.05$). After three weeks, 44 % of the glyphosate disappeared in the BES treatment condition, whereas only 22 % and 16 % decreases were noted under the non-electric and abiotic control conditions, respectively (Fig. 2a, $p < 0.01$). The difference persisted until day 37, where 75 %, 41 %, and 38 % of glyphosate were removed under BES, non-electric control, and abiotic control conditions, respectively (Fig. 2a, $p < 0.001$). The pH decreased to <7.5 after three days in the BES and abiotic control conditions, while a less significant pH reduction was observed under the non-electric control condition (Fig. 2b). The decreasing pH under poised potentials suggested that hydrogen evolution was not a dominant factor in this study.

Second, the BES condition shifted glyphosate degradation towards the C-P lyase pathway. The mole ratio of AMPA produced to glyphosate removed was significantly lower under the BES treatment condition than the other two conditions and decreased throughout the treatment process (Fig. S1). The mole ratio of sarcosine and glycine concentrations to glyphosate removed generally supported the same conclusion, but the difference between BES and non-electric conditions were less pronounced possibly due to biologically sourced or utilized glycine and sarcosine (Fig. S1). The final AMPA yield in this study (i.e., 0.52 mol AMPA yield per mol glyphosate degraded, Table 1), is significantly lower than most of the previous glyphosate biodegradation studies that did not employ electric stimulation (Table 1). The only exception is a study that reported a ratio of 0.15 mol/mol (Ref. (Tang et al., 2019) in Table 1), where the authors applied soil collected from a site with a long history of high glyphosate exposure (i.e., once every three months for four years) and pre-acclimated microbial community (Pizarro et al., 2016; Ratcliff et al., 2006).

The total phosphorus recovery was 156 %–169 % and 182–196 % under the BES treatment and non-electric control conditions respectively, significantly higher than the abiotic control (115 %–129 %) (Fig. 3a). The additional phosphorus is likely sourced from microbial decay and genomic phosphorus, since previous studies reported the toxicity of glyphosate on microbial cells (Roberts et al., 2002; Zablotowicz and Reddy, 2004). The fast kinetics of glyphosate removal under BES condition reduced microbial decay, which led to lower phosphorus recovery than the non-electric control condition (Figs. 3a and S2d). The reason for the increase (15 %–29 %) in phosphorus recovery in the abiotic control was unclear. On day 37, all the catholyte from the abiotic control was filtered with 0.22 μm sterile filter and nucleic acid extraction was performed on the filter membrane. The total DNA yield was <5

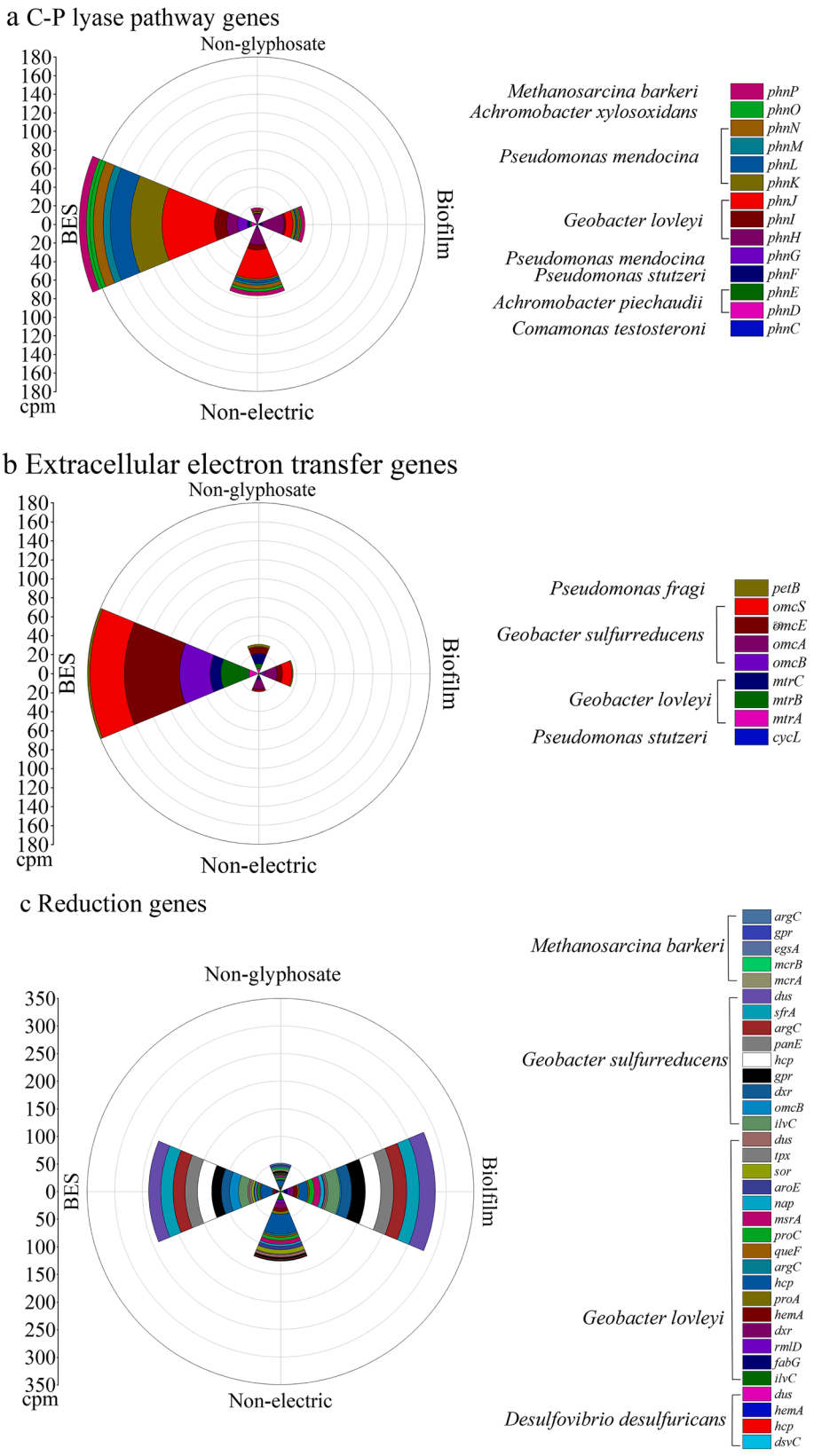

Fig. 5. Abundance of the genes related to C-P lyase (a), electron transfer (b) and reduction (c) functions. "Biofilm", "Non-electric", "BES", and "Non-glyphosate" represent the microbial community at the starting point, and day 37 in the open circuit control condition, the BES treatment condition, and the non-glyphosate control condition respectively. cpm: counts per million.

ng. Therefore, a likely reason was uncontrollable experimental inaccuracies.

The total molar recovery of glyphosate and degradation products was 115 % - 152 % and 116 % - 146 % under the BES treatment and non-electric control conditions respectively, higher than the abiotic control (101 %–140 %) (Fig. 3b). The extra recovery under biological conditions was likely the additional glycine/sarcosine from the metabolic productions of the microbial communities, since glycine/sarcosine-producing microorganisms were detected in the microbial community (Fig. S2).

3.3. Poised potential and Geobacter were significantly correlated with the C-P lyase pathway

In addition to strong correlations with the concentrations of glycine and sarcosine, poised potential increased the relative abundance of *Geobacter lovleyi* and the microbial community diversity as measured by the Shannon diversity indices (Figs. 4 and S2), suggesting that it mitigated the toxicity of glyphosate on microbial communities through faster removal or adaptation (Giesy et al., 2000; Hove-Jensen et al., 2014). The relative abundance of *Geobacter lovleyi* (5.35 %) and *Geobacter* sp. (75.81 %) showed strong correlations with the glyphosate concentrations, while the relative abundance of *Desulfovibrio vulgaris* (3.89 %) was correlated with the concentrations of glycine and sarcosine (Fig. 4). *Geobacter* sp. and *Geobacter lovleyi* are known electro-active species, and strains from *Geobacter lovleyi* are organohalide-respirating bacteria (Wagner et al., 2012). *D. vulgaris*a is strictly anaerobic, sulfate-reducing bacterium with the ability of activating distinct pathways in response to survival stresses (Zhou et al., 2011).

3.4. C-P lyase pathway was likely simulated by the phnJ, mtrB, and hcp genes from Geobacter lovleyi

Genes encoding the necessary proteins for C-P lyase core complex, including *phn*G, *phn*H, *phn*I, *phn*J, *phn*K, *phn*L, and *phn*M (Stosiek et al., 2020), were 2.5–10.8 times higher under the BES condition than non-electric and non-glyphosate conditions (Fig. 5a). Most notably, *phn*J from *Geobacter lovleyi*, the gene encoding the main functional C-P bond cleavage protein (Horsman and Zechel, 2017), was the most abundant *phn* gene under the BES condition (57 cpm), which was 1.8 times of that under the non-electric condition and undetected under the non-glyphosate condition (Fig. 5a). *phn*K and *phnL* from *Pseudomonas mendicina* were the second and third most abundant *phn* gene under the BES condition, also significantly higher than the other conditions (Fig. 5a).

Extracellular electron transfer genes were also significantly up-regulated under the BES condition, with 5.8- and 9.4-times increases noted compared to non-glyphosate and non-electric conditions (Fig. 5b). *omcB, omcS*, and *omcE* from *Geobacter sulfurreducens* were the most abundant extracellular electron transfer genes under the BES condition (32.0 to 57.7 cpm), followed by *mtrB* from *Geobacter lovleyi* (29.6 cpm, Fig. 5b).

Reduction-related genes were generally down-regulated under the BES conditions compared to the biofilm control, but up-regulated compared to non-glyphosate and non-electric conditions. The hydroxylamine reductase (hcp) gene from *Geobacter lovleyi* was the most abundant one (35.6 cpm) under the BES condition, which was 1.7- to 3.2-times higher than the other conditions (Fig. 5c). This agrees with a previous study that suggested significant correlations between hydroxylamine reductase activity and glyphosate degradation in agricultural soil (Chen et al., 2023).

Overall, the results suggest that glyphosate degradation under poised potential was likely catalyzed by *Geobacter lovleyi* given its significantly increased relative abundance (Fig. S2), correlation with glyphosate concentration (Fig. 4), and up-regulation of genes encoding C-P lyase core complex (*phnJ*), extra-cellular electron transfer (*mtrB*), and reduction (*hcp*) (Fig. 5). *Geobacter sulfurreducens,* which was previously reported to be in the microbial consortia in the remediation of soil and water polluted by indiscriminate use of herbicides and pesticides (Behera et al., 2022), likely contributed through facilitating the extracellular electron transfer (Fig. 5) despite the low relative abundance (0.3 % in the BES condition, Fig. S2). *Pseudomonas mendicina*, although also low in relative abundance (0.1 % in the BES condition, Fig. S2), likely contributed to the enhanced C-P lyase pathway as evidenced by the up-regulation of its *phn*K and *phnL* genes (Fig. 5). *Geobacter* sp., while high in relative abundance (Fig. S2) and correlated with glyphosate concentrations (Fig. 4), was not significant in terms of functional gene expression.

4. Conclusions

This study investigated the degradation of glyphosate in bio-electrochemical systems (BES) with cathodic poised potentials. DFT simulations predicted that the C-P lyase degradation pathway would be thermodynamically favorable under external charge. Experimental results confirmed that cathodic poised potentials improved the kinetics of glyphosate degradation up to 200 % of abiotic and open-circuit control conditions, and lowered the AMPA yield by 30 %. The enhanced C-P lyase pathway was likely related to the proliferation of *Geobacter lovleyi,* and the up-regulation of its *phnJ, mtrB* and *hcp* genes. This research shows the potential of BES as a glyphosate treatment process, which could be more affordable than current options (Table S4) while reducing the risk of secondary pollution by lowering the chemical and energy consumption.

CRediT authorship contribution statement

Qingshi Wang: Writing – original draft, Visualization, Investigation, Formal analysis, Data curation. **Jackson Boodry:** Writing – original draft, Visualization, Formal analysis, Data curation. **Tahir Maqbool:** Writing – review & editing, Methodology. **Brandon C. Bukowski:** Writing – review & editing, Methodology, Funding acquisition. **Daqian Jiang:** Writing – review & editing, Project administration, Funding acquisition, Data curation, Conceptualization.

Declaration of competing interest

The authors declare that they have no known competing financial interests or personal relationships that could have appeared to influence the work reported in this paper.

Data availability

Data will be made available on request.

Acknowledgments

DJ acknowledges financial support by the U.S. National Science Foundation (award number 2305141). JB and BCB acknowledge the Advanced Research Computing at Hopkins (ARCH) core facility (rockfish.jhu.edu), which is supported by the National Science Foundation (NSF) grant number OAC1920103. The views and conclusions contained in this document are those of the authors and should not be interpreted as representing the official policies, either expressed or implied. We thank Dr. Qiaoli Liang for the assistance with the LC-MS/MS analysis.

Supplementary materials

Supplementary material associated with this article can be found, in the online version, at doi:10.1016/j.watres.2024.122373.

References

Balbuena, M.S., Tison, L., Hahn, M.L., Greggers, U., Menzel, R., Farina, W.M., 2015. Effects of sublethal doses of glyphosate on honeybee navigation. J. Exp. Biol. 218, 2799–2805. https://doi.org/10.1242/jeb.117291.

Battaglin, W.A., Meyer, M.T., Kuivila, K.M., Dietze, J.E., 2014. Glyphosate and its degradation product AMPA occur frequently and widely in U.S. soils, surface water, groundwater, and precipitation. J. Am. Water Resour. Assoc. 50, 275–290. https://doi.org/10.1111/jawr.12159.

Becke, A.D., 1993. Density-functional thermochemistry. III. The role of exact exchange. J. Chem. Phys. 98, 5648–5652. https://doi.org/10.1063/1.464913.

Becke, A.D., 1988. Density-functional exchange-energy approximation with correct asymptotic behavior. Phys. Rev. A 38, 3098–3100. https://doi.org/10.1103/PhysRevA.38.3098.

Behera, L., Datta, D., Kumar, S., Kumar, S., Sravani, B., Chandra, R., 2022. Role of microbial consortia in remediation of soil, water and environmental pollution caused by indiscriminate use of chemicals in agriculture: opportunities and challenges. New and Future Developments in Microbial Biotechnology and Bioengineering. Elsevier, pp. 399–418. https://doi.org/10.1016/B978-0-323-85577-8.00019-6.

Benbrook, C.M., 2016. Trends in glyphosate herbicide use in the United States and globally. Environ. Sci. Eur. 28, 3. https://doi.org/10.1186/s12302-016-0070-0.

Bento, C.P.M., Yang, X., Gort, G., Xue, S., van Dam, R., Zomer, P., Mol, H.G.J., Ritsema, C.J., Geissen, V., 2016. Persistence of glyphosate and aminomethylphosphonic acid in loess soil under different combinations of temperature, soil moisture and light/darkness. Sci. Total Environ. 572, 301–311. https://doi.org/10.1016/j.scitotenv.2016.07.215.

Bhatt, P., Joshi, T., Bhatt, K., Zhang, W., Huang, Y., Chen, S., 2021. Binding interaction of glyphosate with glyphosate oxidoreductase and C–P lyase: molecular docking and molecular dynamics simulation studies. J. Hazard. Mater. 409, 124927 https://doi.org/10.1016/j.jhazmat.2020.124927.

Brandon, T.A., Stamps, B.W., Cummings, A., Zhang, T., Wang, X., Jiang, D., 2020. Poised potential is not an effective strategy to enhance bio-electrochemical denitrification under cyclic substrate limitations. Sci. Total Environ. 713, 136698 https://doi.org/10.1016/j.scitotenv.2020.136698.

Campanale, C., Massarelli, C., Losacco, D., Bisaccia, D., Triozzi, M., Uricchio, V.F., 2021. The monitoring of pesticides in water matrices and the analytical criticalities: a review. TrAC Trends Anal. Chem. 144, 116423 https://doi.org/10.1016/j.trac.2021.116423.

Chen, Y., Gong, M., Liang, D., Li, S., Meng, D., He, J., Li, Y., Kang, Z., Li, H., 2023. Application of urea hydrogen peroxide: degradation of glyphosate in soil and effect on ammonia nitrogen effectiveness and enzyme activity. J. Environ. Chem. Eng. 11, 110949 https://doi.org/10.1016/j.jece.2023.110949.

Cottrell, T.L., 1958. The Strengths of Chemical Bonds, 2nd ed. Butterworths, London.

Duke, S.O., Powles, S.B., 2008. Glyphosate: a once-in-a-century herbicide: glyphosate: a once-in-a-century herbicide. Pest Manag. Sci. 64, 319–325. https://doi.org/10.1002/ps.1518.

European Food Safety Authority (EFSA), 2015. Conclusion on the Peer Review of the Pesticide Risk Assessment of the Active Substance Glyphosate, 13. EFS2. https://doi.org/10.2903/j.efsa.2015.4302.

Fan, J., Yang, G., Zhao, H., Shi, G., Geng, Y., Hou, T., Tao, K., 2012. Isolation, identification and characterization of a glyphosate-degrading bacterium, Bacillus cereus CB4, from soil. J. Gen. Appl. Microbiol. 58, 263–271. https://doi.org/10.2323/jgam.58.263.

Fu, G., Chen, Y., Li, R., Yuan, X., Liu, C., Li, B., Wan, Y., 2017. Pathway and rate-limiting step of glyphosate degradation by *Aspergillus oryzae* A-F02. Prep. Biochem. Biotechnol. 47, 782–788. https://doi.org/10.1080/10826068.2017.1342260.

Giesy, J.P., Dobson, S., Solomon, K.R., 2000. Ecotoxicological risk assessment for roundup® herbicide. In: Ware, G.W. (Ed.), Reviews of Environmental Contamination and Toxicology, Reviews of Environmental Contamination and Toxicology. Springer New York, New York, NY, pp. 35–120. https://doi.org/10.1007/978-1-4612-1156-3_2.

Grandcoin, A., Piel, S., Baurès, E., 2017. AminoMethylPhosphonic acid (AMPA) in natural waters: its sources, behavior and environmental fate. Water Res. 117, 187–197. https://doi.org/10.1016/j.watres.2017.03.055.

Hadi, F., Mousavi, A., Noghabi, K.A., Tabar, H.G., Salmanian, A.H., 2013. New bacterial strain of the genus *Ochrobactrum* with glyphosate-degrading activity. J. Environ. Sci. Health B 48, 208–213. https://doi.org/10.1080/03601234.2013.730319.

Horsman, G.P., Zechel, D.L., 2017. Phosphonate biochemistry. Chem. Rev. 117, 5704–5783. https://doi.org/10.1021/acs.chemrev.6b00536.

Hove-Jensen, B., Zechel, D.L., Jochimsen, B., 2014. Utilization of glyphosate as phosphate source: biochemistry and genetics of bacterial carbon-phosphorus lyase. Microbiol. Mol. Biol. Rev. 78, 176–197. https://doi.org/10.1128/MMBR.00040-13.

Huang, L., Wang, Q., Jiang, L., Zhou, P., Quan, X., Logan, B.E., 2015. Adaptively evolving bacterial communities for complete and selective reduction of Cr(VI), Cu(II), and Cd (II) in biocathode bioelectrochemical systems. Environ. Sci. Technol. 49, 9914–9924. https://doi.org/10.1021/acs.est.5b00191.

IARC, 2015. Evaluation of Five Organophosphate Insecticides and Herbicides (No. 112). IARC Monographs.

Imfeld, G., Lefrancq, M., Maillard, E., Payraudeau, S., 2013. Transport and attenuation of dissolved glyphosate and AMPA in a stormwater wetland. Chemosphere 90, 1333–1339. https://doi.org/10.1016/j.chemosphere.2012.04.054.

Jacob, G.S., Garbow, J.R., Hallas, L.E., Kimack, N.M., Kishore, G.M., Schaefer, J., 1988. Metabolism of glyphosate in Pseudomonas sp. strain LBr. Appl. Environ. Microbiol. 54, 2953–2958. https://doi.org/10.1128/aem.54.12.2953-2958.1988.

Kosar, B., Albayrak, C., 2011. Spectroscopic investigations and quantum chemical computational study of (E)-4-methoxy-2-[(p-tolylimino)methyl]phenol. Spectrochim. Acta A: Mol. Biomol. Spectrosc. 78, 160–167. https://doi.org/10.1016/j.saa.2010.09.016.

Krzyśko-Lupicka, T., Strof, W., Kubś, K., Skorupa, M., Wieczorek, P., Lejczak, B., Kafarski, P., 1997. The ability of soil-borne fungi to degrade organophosphonate carbon-to-phosphorus bonds. Appl. Microbiol. Biotechnol. 48, 549–552. https://doi.org/10.1007/s002530051095.

Lehtola, S., Steigemann, C., Oliveira, M.J.T., Marques, M.A.L., 2018. Recent developments in libxc — A comprehensive library of functionals for density functional theory. SoftwareX 7, 1–5. https://doi.org/10.1016/j.softx.2017.11.002.

Logan, B.E., Call, D., Cheng, S., Hamelers, H.V.M., Sleutels, T.H.J.A., Jeremiasse, A.W., Rozendal, R.A., 2008. Microbial electrolysis cells for high yield hydrogen gas production from organic matter. Environ. Sci. Technol. 42, 8630–8640. https://doi.org/10.1021/es801553z.

Musa, E.N., Kaur, S., Gallagher, T.C., Anthony, T.M., Stickle, W.F., Árnadóttir, L., Stylianou, K.C., 2023. Two birds, one stone: coupling hydrogen production with herbicide degradation over metal–organic framework-derived titanium dioxide. ACS Catal. 13, 3710–3722. https://doi.org/10.1021/acscatal.3c00265.

Neese F., 2018. Software update: the ORCA program system, version 4.0. WIREs Comput Mol Sci 8, e1327. 10.1002/wcms.1327.

Neese, F., 2012. The ORCA program system. WIREs Comput. Mol. Sci. 2, 73–78. https://doi.org/10.1002/wcms.81.

Obojska, A., Ternan, N.G., Lejczak, B., Kafarski, P., McMullan, G., 2002. Organophosphonate Utilization by the Thermophile *Geobacillus caldoxylosilyticus* T20. Appl. Environ. Microbiol. 68, 2081–2084. https://doi.org/10.1128/AEM.68.4.2081-2084.2002.

Ololade, I.A., Oladoja, N.A., Oloye, F.F., Alomaja, F., Akerele, D.D., Iwaye, J., Aikpokpodion, P., 2014. Sorption of glyphosate on soil components: the roles of metal oxides and organic materials. soil and sediment contamination. Int. J. 23, 571–585. https://doi.org/10.1080/15320383.2014.846900.

Ololade, O.O., Aiyesanmi, A.F., Okoronkwo, A.E., Adanigbo, P., Ololade, I.A., 2019. Influence of cow-dung amendment on glyphosate mobility in soil. Toxicol. Environ. Chem. 101, 265–280. https://doi.org/10.1080/02772248.2019.1662018.

Pant, D., Singh, A., Van Bogaert, G., Irving Olsen, S., Singh Nigam, P., Diels, L., Vanbroekhoven, K., 2012. Bioelectrochemical systems (BES) for sustainable energy production and product recovery from organic wastes and industrial wastewaters. RSC Adv. 2, 1248–1263. https://doi.org/10.1039/C1RA00839K.

Pizarro, H., Vera, M.S., Vinocur, A., Pérez, G., Ferraro, M., Menéndez Helman, R.J., Dos Santos Afonso, M., 2016. Glyphosate input modifies microbial community structure in clear and turbid freshwater systems. Environ. Sci. Pollut. Res. 23, 5143–5153. https://doi.org/10.1007/s11356-015-5748-0.

Ratcliff, A.W., Busse, M.D., Shestak, C.J., 2006. Changes in microbial community structure following herbicide (glyphosate) additions to forest soils. Appl. Soil Ecol. 34, 114–124. https://doi.org/10.1016/j.apsoil.2006.03.002.

Roberts, C.W., Roberts, F., Lyons, R.E., Kirisits, M.J., Mui, E.J., Finnerty, J., Johnson, J.J., Ferguson, D.J.P., Coggins, J.R., Krell, T., Coombs, G.H., Milhous, W.K., Kyle, D.E., Tzipori, S., Barnwell, J., Dame, J.B., Carlton, J., McLeod, R., 2002. The shikimate pathway and its branches in apicomplexan parasites. J. Infect. Dis. 185, S25–S36. https://doi.org/10.1086/338004.

Romano-Armada, N., Amoroso, M.J., Rajal, V.B., 2019. Construction of a combined soil quality indicator to assess the effect of glyphosate application. Sci. Total Environ. 682, 639–649.

Scribner E.A., Battaglin W.A., Gilliom R.J., Meyer M.T., 2007. Concentrations of glyphosate, its degradation product, aminomethylphosphonic acid, and glufosinate in ground- and surface-water, rainfall, and soil samples collected in the United States, 2001–06.

Sevda, S., Sreekishnan, T.R., Pous, N., Puig, S., Pant, D., 2018. Bioelectroremediation of perchlorate and nitrate contaminated water: a review. Bioresour. Technol. 255, 331–339. https://doi.org/10.1016/j.biortech.2018.02.005.

Silva, V., Montanarella, L., Jones, A., Fernández-Ugalde, O., Mol, H.G.J., Ritsema, C.J., Geissen, V., 2018. Distribution of glyphosate and aminomethylphosphonic acid (AMPA) in agricultural topsoils of the European Union. Sci. Total Environ. 621, 1352–1359. https://doi.org/10.1016/j.scitotenv.2017.10.093.

Stephens, P.J., Devlin, F.J., Chabalowski, C.F., Frisch, M.J., 1994. Ab initio calculation of vibrational absorption and circular dichroism spectra using density functional force fields. J. Phys. Chem. 98, 11623–11627. https://doi.org/10.1021/j100096a001.

Stosiek, N., Talma, M., Klimek-Ochab, M., 2020. Carbon-phosphorus lyase—the state of the art. Appl. Biochem. Biotechnol. 190, 1525–1552. https://doi.org/10.1007/s12010-019-03161-4.

Sun, M., Li, H., Jaisi, D.P., 2019. Degradation of glyphosate and bioavailability of phosphorus derived from glyphosate in a soil-water system. Water Res. 163, 114840 https://doi.org/10.1016/j.watres.2019.07.007.

Sviridov, A.V., Shushkova, T.V., Zelenkova, N.F., Vinokurova, N.G., Morgunov, I.G., Ermakova, I.T., Leontievsky, A.A., 2012. Distribution of glyphosate and methylphosphonate catabolism systems in soil bacteria Ochrobactrum anthropi and Achromobacter sp. Appl. Microbiol. Biotechnol. 93, 787–796. https://doi.org/10.1007/s00253-011-3485-y.

Tang, F.H.M., Jeffries, T.C., Vervoort, R.W., Conoley, C., Coleman, N.V., Maggi, F., 2019. Microcosm experiments and kinetic modeling of glyphosate biodegradation in soils and sediments. Sci. Total Environ. 658, 105–115. https://doi.org/10.1016/j.scitotenv.2018.12.179.

Torretta, V., Katsoyiannis, I., Viotti, P., Rada, E., 2018. Critical review of the effects of glyphosate exposure to the environment and humans through the food supply chain. Sustainability 10, 950. https://doi.org/10.3390/su10040950.

Van Bruggen, A.H.C., He, M.M., Shin, K., Mai, V., Jeong, K.C., Finckh, M.R., Morris, J.G., 2018. Environmental and health effects of the herbicide glyphosate. Sci. Total Environ. 616–617, 255–268. https://doi.org/10.1016/j.scitotenv.2017.10.309.

Villano, M., Aulenta, F., Ciucci, C., Ferri, T., Giuliano, A., Majone, M., 2010. Bioelectrochemical reduction of CO2 to CH4 via direct and indirect extracellular electron transfer by a hydrogenophilic methanogenic culture. Bioresour. Technol. 101, 3085–3090. https://doi.org/10.1016/j.biortech.2009.12.077.

Wagner, D.D., Hug, L.A., Hatt, J.K., Spitzmiller, M.R., Padilla-Crespo, E., Ritalahti, K.M., Edwards, E.A., Konstantinidis, K.T., Löffler, F.E., 2012. Genomic determinants of organohalide-respiration in Geobacter lovleyi, an unusual member of the Geobacteraceae. BMC Genom. 13, 200. https://doi.org/10.1186/1471-2164-13-200.

Weigend, F., Ahlrichs, R., 2005. Balanced basis sets of split valence, triple zeta valence and quadruple zeta valence quality for H to Rn: design and assessment of accuracy. Phys. Chem. Chem. Phys. 7, 3297. https://doi.org/10.1039/b508541a.

Wilberforce, T., Sayed, E.T., Abdelkareem, M.A., Elsaid, K., Olabi, A.G., 2021. Value added products from wastewater using bioelectrochemical systems: current trends and perspectives. J. Water Process. Eng. 39, 101737 https://doi.org/10.1016/j.jwpe.2020.101737.

Zablotowicz, R.M., Reddy, K.N., 2004. Impact of glyphosate on the symbiosis with glyphosate-resistant transgenic soybean. J. Environ. Qual. 33, 825. https://doi.org/10.2134/jeq2004.0825.

Zhan, H., Feng, Y., Fan, X., Chen, S., 2018. Recent advances in glyphosate biodegradation. Appl. Microbiol. Biotechnol. 102, 5033–5043. https://doi.org/10.1007/s00253-018-9035-0.

Zhang, C., Hu, X., Luo, J., Wu, Z., Wang, L., Li, B., Wang, Y., Sun, G., 2015. Degradation dynamics of glyphosate in different types of citrus orchard soils in China. Molecules 20, 1161–1175. https://doi.org/10.3390/molecules20011161.

Zhao, J., Pacenka, S., Wu, J., Richards, B.K., Steenhuis, T., Simpson, K., Hay, A.G., 2018. Detection of glyphosate residues in companion animal feeds. Environ. Pollut. 243, 1113–1118. https://doi.org/10.1016/j.envpol.2018.08.100.

Zhao, Y., Truhlar, D.G., 2008. The M06 suite of density functionals for main group thermochemistry, thermochemical kinetics, noncovalent interactions, excited states, and transition elements: two new functionals and systematic testing of four M06-class functionals and 12 other functionals. Theor. Chem. Account. 120, 215–241. https://doi.org/10.1007/s00214-007-0310-x.

Zhou, J., He, Q., Hemme, C.L., Mukhopadhyay, A., Hillesland, K., Zhou, A., He, Z., Van Nostrand, J.D., Hazen, T.C., Stahl, D.A., Wall, J.D., Arkin, A.P., 2011. How sulphate-reducing microorganisms cope with stress: lessons from systems biology. Nat. Rev. Microbiol. 9, 452–466. https://doi.org/10.1038/nrmicro2575.